Journal of
Nanoscience and Nanotechnology
Vol. 13, 1–10, 2013

Scratch and Abrasion Properties of Polyurethane-Based Micro- and Nano-Hybrid Obturation Materials

Miriam Estevez[1], J. Rogelio Rodriguez[1], Susana Vargas[1], J. A. Guerra[1,2], Witold Brostow[3,*], and Haley E. Hagg Lobland[3]

[1] *Centro de Fisica Aplicada y Tecnología Avanzada (CFATA), Universidad Nacional Autonoma de Mexico, Campus Juriquilla, Queretato, CP 76230, Mexico*
[2] *Posgrado en Ciencia e Ingeniería de Materiales (PCeIM), Universidad Nacional Autonoma de Mexico, Mexico, D.F., Mexico*
[3] *Laboratory of Advanced Polymers and Optimized Materials (LAPOM), Department of Materials Science and Engineering, UNT, 1150 Union Circle # 305310, Denton, TX 76203-5017, USA*

Polyurethane-based micro- and nano-hybrid composites were produced with controlled porosity to be used as obturation materials. In addition to hydroxyapatite (HAp) micro-particles in the composites, two different ceramics particle types were also added: alumina micro-particles and silica nano-particles. Particles of different sizes provide the materials with improved mechanical properties: the use of micro- and nano-particles produces a better packing because the nano-particles fill the interstitial space left by the micro-particles, rendering an improvement in the mechanical properties. The silica and alumina particles provide the materials with appropriate abrasion and scratching properties, while the HAp provides the required bio-acceptance. The polymeric matrix was a mono-component solvent-free polyurethane. The porosity was selected by controlling the chemical reaction.

Keywords: Nanohybrid, Micro-Hybrid, Composite, Hydroxyapatite, Alumina, Silica, Polyurethane, Obturation Materials.

RESEARCH ARTICLE

1. INTRODUCTION

While there is much research on development of biomaterials, the creation of materials capable of tooth ingrowth often receives less attention. There exist a variety of obturation materials—both ceramics and polymeric resin-based composites—for filling dental caries, but most of these are not designed to *interact* with the tooth. In a review of resin-based dental materials, Jandt and Sigusch state the following:

> The main purpose of resin-based restorative materials, such as composites, is to replace lost tooth structure and function with an esthetically pleasing result. These conventional composites, however, have little in common with natural tooth structure and do not support any kind of tissue regeneration. Nevertheless, natural dental tissues possess much better properties and more suitable structures to fulfil their tasks, than the best restorative composite. It is, therefore, interesting to incorporate tissue regenerative properties in dental composites.[1]

For these reasons, we have been working on the development of porous composites for repairing dental caries.[2–5] Several options have been pursued already, with performance near to that of some commercial resins.[2] Here we provide results for more compositions as we aim to develop a better performing formulation.

The obturation materials addressed in this work are polymer+ceramic composites. When ceramic particles are added to a polymeric matrix, the mechanical properties of the composite are generally improved.[6–10] This is especially true if the ceramic-polymer interface is properly controlled. Synergy between two different materials can be obtained if a good transfer of properties through the interfaces is provided.[11,12] Toward that end, polymer-based hybrid organic-inorganic materials have been created. The development and properties of such materials have been reviewed.[13] More specifically, the use of ceramics in biomaterials is addressed by Saenz and colleagues.[14]

The *size* of the discrete phase in a composite also plays an important role in overall performance. For instance, nano-particles provide larger contact area, which in some cases improves property transfer.[15–17] Micro-particles can also be incorporated into polymer-based materials (PBMs)

*Author to whom correspondence should be addressed.

with advantageous effects on mechanical and tribological properties.[18–23] The use of micro- and nano-particles in combination may produce an additional improvement in the performance of the composite if the nano-particles can fill the interstitial space between micro-particles thereby increasing the density. To achieve these effects, it has been shown by some that the particles must be added in order of size: first the micro-particles and then the nano-particles. This has been demonstrated in several cases for composites with silica nano-particles.[24–25] An additional contributing mechanism may involve homogenization of the stress field as described in work by Zhang et al.[26] Zhang and co-authors describe how the use of multiscale ceramic fillers (i.e., both nano and micro fillers) may work synergistically to improve mechanical properties. Moreover, our approach, like that of others,[27] involves novel means of incorporating nanostructures and nanoparticles into materials for bio-related applications.

Two key elements for the allowance of tooth ingrowth are presence of hydroxyapatite and existence of porosity. Composites used as dental obturation materials typically have hydroxyapatite (HAp) as a constituent in order to provide better bio-acceptance.[28] However additional reinforcement is usually necessary because teeth are subjected to strong and continuous stresses and scratches during mastication as well as during tooth brushing. Toothpaste is known to contain abrasive particles. Considering the high demands for dental obturation materials, we have developed a variety of composites, evaluating both mechanical and tribological properties.[3–5] The repetitive intense stresses and scratches to which teeth are exposed can produce fatigue in obturation materials that results in premature wear with the concomitant production of cracks and fissures that act as host sites for bacterial growth.[29–31] It is critical then to improve not only the mechanical performance but also importantly the tribological properties of new obturation materials.[2, 32, 33] Brittleness is also a concern.[34, 35] To address these issues, we have prepared obturation materials containing alumina micro-particles (2.7 μm) and silica nano-particles (16 nm) as reinforcements, along the lines of work reported in Refs. [36, 37].

The dental composites addressed here are based on a polyurethane (PU) resin. The polymeric matrix of the obturation materials is a waterborne mono-component polyurethane not requiring the use of potentially toxic solvents[38, 39] and therefore offering a clear advantage for use in dental systems. The aliphatic (acrylic) hydroxylated resin is mixed with a malonate-blocked polyisocyanate as curing agent. A polyurethane is used because, by itself, it is a highly abrasion resistant polymer with a high agglutination capacity and with the potential to generate a controllably porous material. The presence of cyano groups (from the curing agent), which can react chemically with all the OH groups present in the system (in dentin, HAp, alumina and silica particles), assures a good adherence to the substrate, creates an internal network by linking all components together, and thereby improves the mechanical and tribological properties[29–31] while reducing microfiltration.[40–42]

Porous materials including foams have been widely used from long ago in many technological and industrial applications.[43–48] However, porous biomaterials have recently acquired prominence because they allow one to reproduce the morphology of real bone or teeth in order to fabricate prostheses, implants and obturation materials.[49, 50] In the present case, porosity is controlled through a chemical reaction: when the malonate-blocked polyisocyanate reacts with the hydroxyl groups of all other constituents, part of the blocking structure is released producing CO_2 gas that forms pores.[51, 52] The ceramic particles in the composite provide the effective reaction area and also determine the number of –OH groups available for the reaction. By adjusting the polyisocyanate concentration and the ceramic particle size, the pore size and pore volume fraction can be controlled. In this way it is possible for us to produce a biomaterial with the desired morphology.[53, 54] Moreover, the crosslinking reaction links together the ceramic particles through bridges of polymer molecules, producing an inner network in the material that improves significantly the mechanical and tribological properties.[55, 56] In this work several porous obturation materials were prepared at different concentrations of the ceramic particles.

2. EXPERIMENTAL DETAILS

2.1. Materials

The solvent-free mono-component polyurethane was an aliphatic (acrylic) hydroxylated resin (Bayer) containing a malonate-blocked polyisocyanate in a volume proportion 4:1. Our polyisocyanate cross-linker contains a blocking functionality that limits its own chemical reactivity, thereby stabilizing the resin-plus-isocyanate mixture. In the presence of moisture, part of the blocking structure is released, producing, in this particular case, CO_2, while the rest reacts with –OH groups that are present in the material (e.g., on HAp, the hydroxylated PU resin). Synthetic hydroxyapatite (HAp) was prepared by the method described in Ref. [57] and ground in an agate mortar to a nominal particle size of 1.9 microns. Ceramic particles used were alumina micro-particles (Cabot, USA) and silica nano-particles (Degussa, Germany), with nominal particle diameters of 2.7 microns and 16 nm, respectively.

2.2. Sample Preparation

Five different sample types were prepared with varied amounts of ceramic particles. For each sample, the solvent-free mono-component polyurethane was mixed with the ceramic particles until a homogeneous paste was obtained. The particles were added slowly in order of

Table I. Chemical composition and pore size of all samples.

Sample	PU	HAp	Al_2O_3	SiO_2	Pore Size
RH	8 g	8 g	0 g	0 g	(60 ± 5) μm
RS	8 g	0 g	0 g	8 g	(75 ± 5) μm
RA7S3	8 g	0 g	5.6 g	2.4 g	(82 ± 10) μm
RH7S3	8 g	5.6 g	0 g	2.4 g	(150 ± 10) μm
RA3S3H3	8 g	2.64 g	2.64 g	2.64 g	(75 ± 8) μm

decreasing particle size. Thus, for samples containing all three ceramics, alumina was added first, then HAp followed by silica. The compositions of the prepared samples are reported in Table I. Disks of each sample type were prepared by placing the PU + ceramics paste in a cylindrical Teflon mold 3 mm thick and 2.5 cm in diameter. Samples were allowed to cure for 24 h before beginning characterization. Five disks were prepared for each formulation.

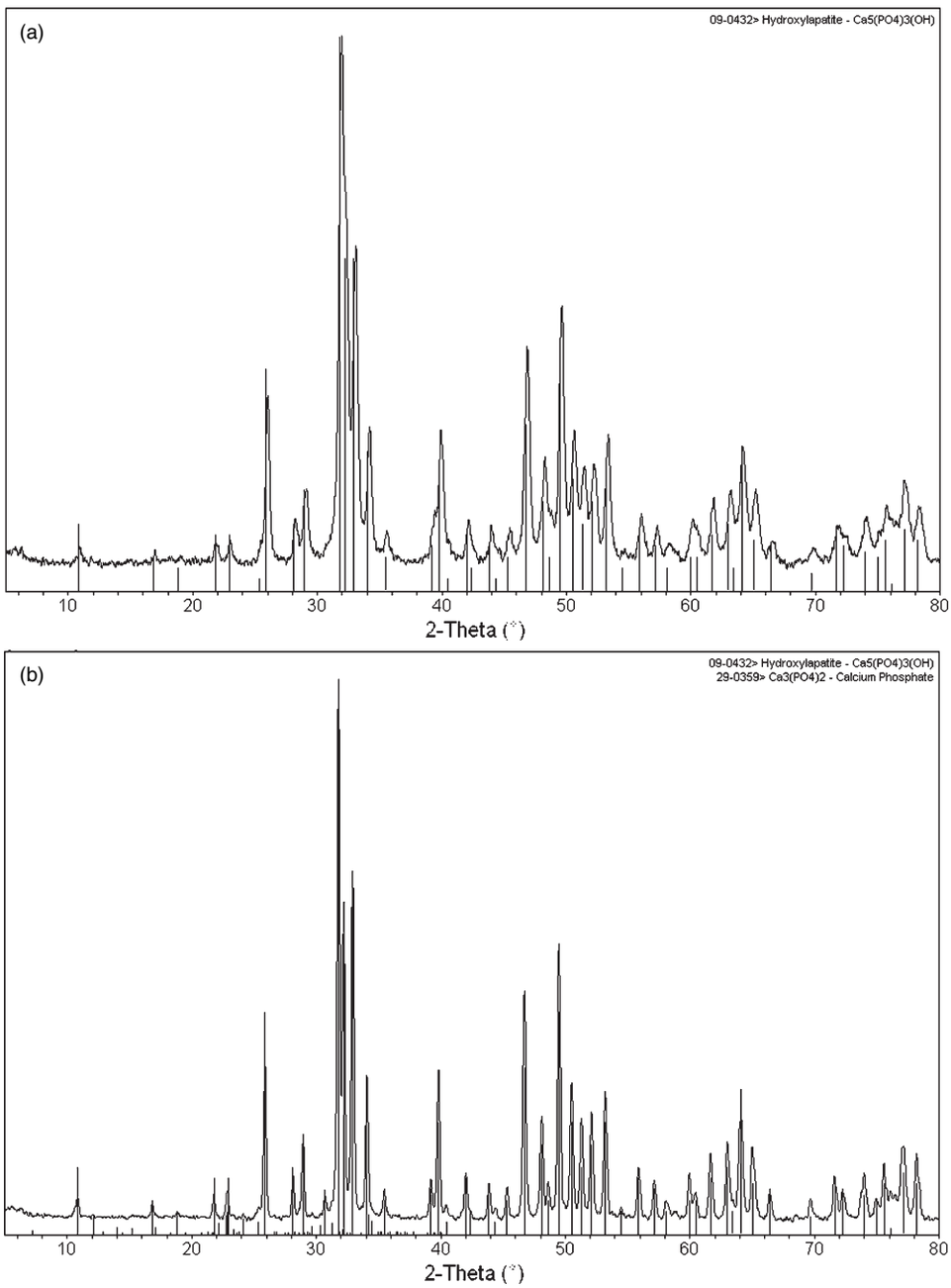

Fig. 1. X-ray diffraction pattern of synthetic HAp: (a) heated at 700 °C during 12 h and (b) heated at 900 °C during 15 h.

RESEARCH ARTICLE

2.3. Characterization

2.3.1. Particle Size

The particle size of the ceramic particles was determined using a dynamic light scattering (DLS) apparatus (Brookhaven Instruments Corp., model BI-APD) equipped with a He-Ne laser at 632.8 nm and a digital correlator obtaining 16 nm for silica and 2.7 microns for alumina. The particle size of HAp (1.9 microns) was determined by the same method.

2.3.2. HAp Analysis

The X-ray Diffraction (XRD) patterns of HAp were obtained using a Rigaku D500 machine with a radiation source of 0.154 nm (Cu K_a line); the angle 2θ was varied from 5° to 80° at a scan rate of 2°/min. The stoichiometric ratio Ca/P for the synthetic HAp was determined using the Induced Coupled Plasma Optical Emission Spectroscopy (ICP-OES) with a Thermo Scientific apparatus (model iCAP series 6000). First the HAp was digested with nitric acid in a Mars Xpress CEM digester oven: 0.1 g of HAp was mixed with 7 mL of HNO_3 (grade INSTRA) and the mixture brought to 100 mL with distilled water. Following the digestion, specimens were heated for various periods of time. The selected temperatures were 60, 100, 150 and 190 °C and the corresponding holding times were 5, 10, 10 and 15 min; the heating rate was 4 °C/min. Specimens were then kept at 7 °C during 5 days after which they were tested by ICP-OES and the proper stoichiometry confirmed. Finally, FT-IR analysis of the HAp was performed in a Bruker model Alpha-T Spectrometer equipped with Diffuse Reflectance (DR) and Attenuated Total Reflectance (ATR).

2.3.3. Mechanical Testing and Morphology

Scanning Electron Microscopy (SEM) of the prepared obturation materials was performed in a JEOL JSM-6060 at 20 kV in secondary electron mode with different magnifications. Specimens were frozen in liquid N_2 and then broken, and the newly exposed surface was covered with a gold film. Mechanical tests were conducted in an Adamel Lhomargy machine model DY.22 in compression mode according to ASTM D-695-02a; the compression rate was 1.3 mm/min.

2.3.4. Abrasion Testing

Wear resistance was determined using the Taber Method according to ASTM standard D-1242.[58] Samples were abraded by F-120 Fandeli sandpaper mounted on a steel plate rotating at 250 rpm in dry conditions; the samples were loaded with a weight of 10 g. The weight of specimens before and after abrasion was recorded to determine the weight loss and therefore wear resistance. The weight loss was determined every 20 seconds with an accuracy of $\pm 1 \times 10^{-5}$ g. After the sanding procedure and before the weight determination, the scratched surface was wiped clean with a dry, soft cloth to remove the dust; the sand paper was also cleaned with a soft brush. Five of such experiments were conducted for each sample type, all at room temperature.

2.3.5. Scratch Testing

Scratching behavior (in both progressive and multiple pass scratch experiments) was evaluated through use of a Micro-Scratch Tester (MST) (CSEM Instruments, Neuchatel, Switzerland). The indenter was a Rockwell diamond tip with a 200 μm radius. A pre-scan and post-scan

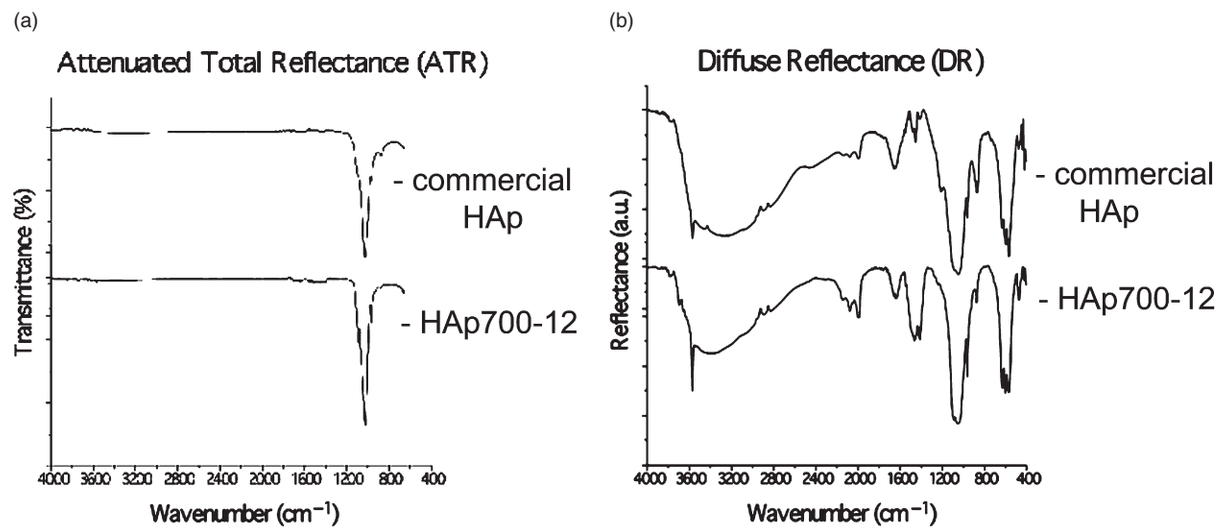

Fig. 2. FT-IR of synthetic and commercial HAp: (a) ATR spectra and (b) DR spectra.

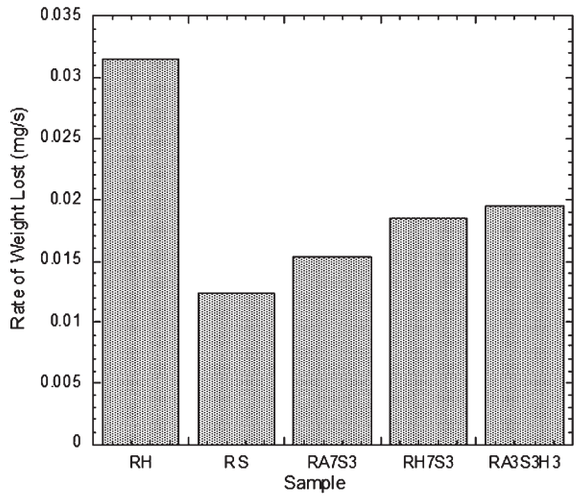

Fig. 3. Rate of lost weight in abrasion experiments for all samples.

were performed in each experiment: the pre-scan to characterize the topography of the surface to be scratched and the post-scan to determine the residual depth. The penetration depth (P_d), a measure of the depth of the scratch groove, and the residual depth (R_d), a measure of the groove depth after the scratching process was completed, were measured directly with the MST machine. From the residual depth and penetration depth, the percentage of recovery ($R_{\%}$) (healing) of the samples was calculated according to the equation: $R_{\%} = [1 - R_d/P_d]\ 100\%$.[59] The recovery was calculated for both progressive and multiple pass scratch tests. Multiple pass (i.e., sliding wear) scratch tests consisted of fifteen consecutive 5.0 mm scratches along the same groove[60–63] at a load of 5.0 N and with a scratch speed of 5.0 mm/min. For the progressive scratch tests, an incremental load from 5.0 to 30.0 N was applied over a single pass at a rate of 5.0 N/min over a length of 5.0 mm. Both scratch test types were run in triplicate for each sample type and the averages calculated.

3. RESULTS

During the HAp synthesis, an excess of 9% of Ca was used in order to obtain the desired phase and the proper stoichiometric Ca/P ratio. Figure 1(a) shows the X-ray diffractogram of a HAp sample heated at 700 °C during 12 h (the treatment used for HAp in the obturation materials). By analysis using MDI JADE 5.0 software, it is clear that the only phase present is HAp. It has been reported that if the temperature and/or the heating time are increased, a new phase, namely tri-calcium phosphate ($Ca_3(PO_4)_2$), will appear.[64–67] Actually, HAp and tri-calcium phosphate phases have similar characteristic peaks. We see that Figure 1(b) for the higher temperature has narrower peaks than Figure 1(a)–while the peak positions and relative peak intensities are very similar. This suggests higher crystallinity (larger crystal grains)–explicable by crystal growth and/or the phase transition seen by earlier researchers. The Ca/P ratio determined by Induced Coupled Plasma Optical Emission Spectroscopy was 1.679, very close to the stoichiometric value (1.667).

The FT-IR spectra (by ATR and DR techniques) of our synthetic HAp (HAp-700-12, which was heated 12 h. at 700 °C and was the type used in sample preparation) and commercial HAp are compared in Figures 2(a) and (b). Several bands are visible in the ATR spectrum of Figure 2(a): the bands at 963 and 1026 cm^{-1} correspond to the symmetric and asymmetric stretching vibration of the P–O group; a band at 1088 cm^{-1} corresponds to the asymmetric stretching vibration of the P═O group; and the band at 3571 cm^{-1} corresponds to the stretching vibration of the O–H group. The following are observed in the DR spectra of Figure 2(b): bands at 569, 602 and 632 cm^{-1}

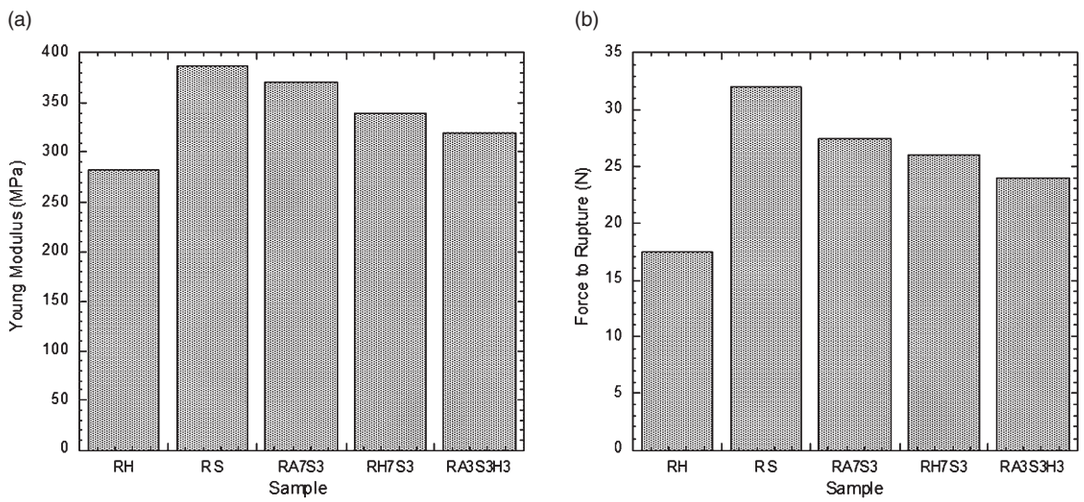

Fig. 4. Results of the mechanical tests: (a) Young modulus and (b) force to rupture.

corresponding to the scissoring vibration of the O–P–O group; a band at 963 cm^{-1} corresponding to the symmetric stretching vibration of the P–O group; and bands at 1053 and 1090 cm^{-1} corresponding to the asymmetric stretching vibration of the same P–O group.

The abrasion results for the composites (see Table I for compositions) prepared are shown in Figure 3. From these results it is evident that the most abrasion-resistant material was the one containing silica (RS), which had the lowest weight loss rate. Although slightly less resistant than the sample containing silica alone, the sample containing all three ceramics (RA3S3H3) was markedly more wear-resistant than the polymer resin with only HAp as a filler.

Young's compression modulae are reported in Figure 4(a). At less than 300 MPa, the Young's modulus of sample RH (resin + HAp) is the lowest. The modulus for the remaining samples—RA3S3H3, RH7S3, RA7S3, RS is greater than 300 MPa.

In Figure 4(b) we present force-to-rupture values. A simple comparison of Figure 4(a) with 4(b) shows that the pattern is qualitatively the same. We see the highest compressive modulus and the highest force to rupture for the RS sample while the lowest values of both quantities pertain to the RH sample.

Again, sample names and compositions are described in Table I. The SEM micrographs are reported in Figures 5(a) through 5(e) and the pore sizes in Table I. Figure 5(a) corresponds to sample RH (100% of filler is HAp), showing interconnected pores with a size of (60 ± 5) microns, the smallest average pore size of all the sample types. The image in Figure 5(b) corresponds to the sample containing 100% silica nano-particles as filler in the PU matrix (RS); the size of the interconnected pores is (75 ± 5) microns. SEM images for samples RA7S3 and RH7S3 are reported in Figures 5(c) and (d); the pore sizes for these samples are (82 ± 10) and (150 ± 10) microns, respectively, and contain some small closed pores (not interconnected). The sample RA3S3H3 (Fig. 5(e)) had an average pore size of (75 ± 8) microns; most pores appeared interconnected with only a few closed pores present.

The scratching results are reported in Figures 6(a) to (c) for sliding wear—that is multiple pass scratch (MPS) tests—and in Figures 7(a) to (c) for progressive scratch (PS) tests. Figure 6(a) shows the penetration depth from MPS tests as a function of the scratch number. With the exception of RH7S3, the penetration depth does not change appreciably with increasing number of scratches. The sample with the highest scratching resistance was RH where the penetration depth ranged between 54 μm for the first scratch and 69 μm for the fifteenth. The samples RS and RA3S3H3 had constant depths of approximately 120 and 128 μm, respectively. The sample RH7S3 showed a significant depth increase from 110 to 160 μm with the number of scratches, while the sample RA7S3 had a practically constant penetration depth with values between 140 and 150 μm. The low values for RH can be explained by returning to Figure 5. We see in Figure 5(a) that RH has the smallest average pore size among all samples investigated. Given the earlier results of abrasion and mechanical testing, the low penetration depth of RH cannot be accounted for by hardness or high strength but rather seems to be largely the result of porosity. Apparently smaller pores offer more resistance while larger pores facilitate the work of the indenter resulting in deeper overall penetration—therefore giving us a pore-facilitation model of scratch behavior. Since consecutive runs after the first one follow the original groove, they do not affect further the situation in a significant way. We recall our work using a profilometer and Vickers hardness determination[60] and microindentation of the grooves and their surroundings.[61] Consecutive scratching runs result among other effects in densification of the material below the groove surface.[60, 61]

Like the penetration depth, the residual depth was also recorded from MPS tests. The residual depth of samples RH7S3 and RA7S3 spanned a wide range: from 54 to 110 μm and from 47 to 85 μm, respectively, between the

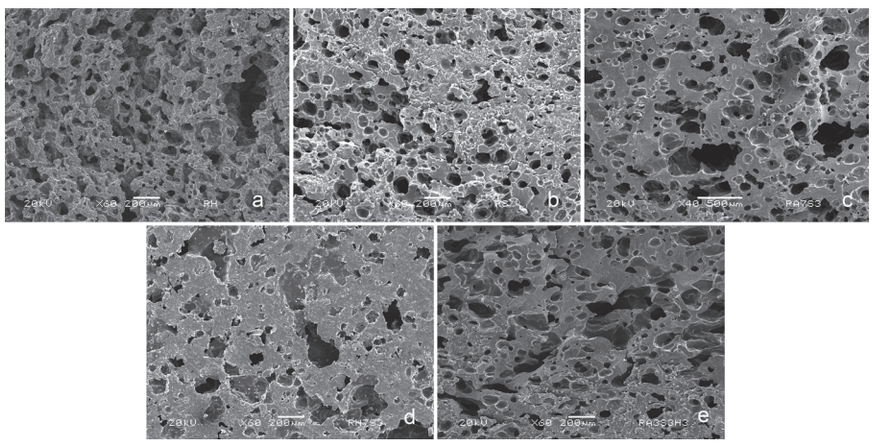

Fig. 5. SEM images for the samples: (a) RH, (b) RS, (c) RA7S3, (d) RH7S3 and (e) RA3S3H3.

RESEARCH ARTICLE

first and fifteenth scratch. In all cases we see a tendency to reach an asymptote so that after a certain number of scratches the depth of the groove does not change anymore. This is the phenomenon of strain hardening in sliding wear discovered in Ref. [62], confirmed since[63] and one of the reasons for formulating a quantitative definition of brittleness.[34]

Given strain hardening, the percentage of recovery (Fig. 6(c)) is reduced as the number of scratches is increased. The samples with the smallest increment of change in residual depth were RS and RA3S3H3; consequently, for these samples, the highest percentage of recovery was obtained (Fig. 6(c)). The samples with the lowest recovery were RH and RH7S3.

Figure 7(a) shows the penetration depths for the progressive scratch tests, conducted over a range of loads between 5.0 N and 30.0 N. At low load (5 N) the penetration depths are between 50 and 125 μm. As the load increases, the spread of the penetration values increases, finally spanning a range from 250 to 400 μm (at 30 N). For all sample types, the penetration depth increases approximately linearly with the load. Samples RH and RA7S3 were penetrated least while samples RS and RA3S3H3 had the highest penetration values. The residual depths are reported in Figure 7(b)—where similar behavior is observed. As with the penetration depth, the residual depth increases approximately linearly with the load. Consequently, as seen in Figure 7(c), the recovery values are practically independent of the load, especially for loads higher than 10 N. The percentage of recovery for RS is nearly constant (60%) while the recovery for each of the other samples spans a relatively small range of values (all less than 62%).

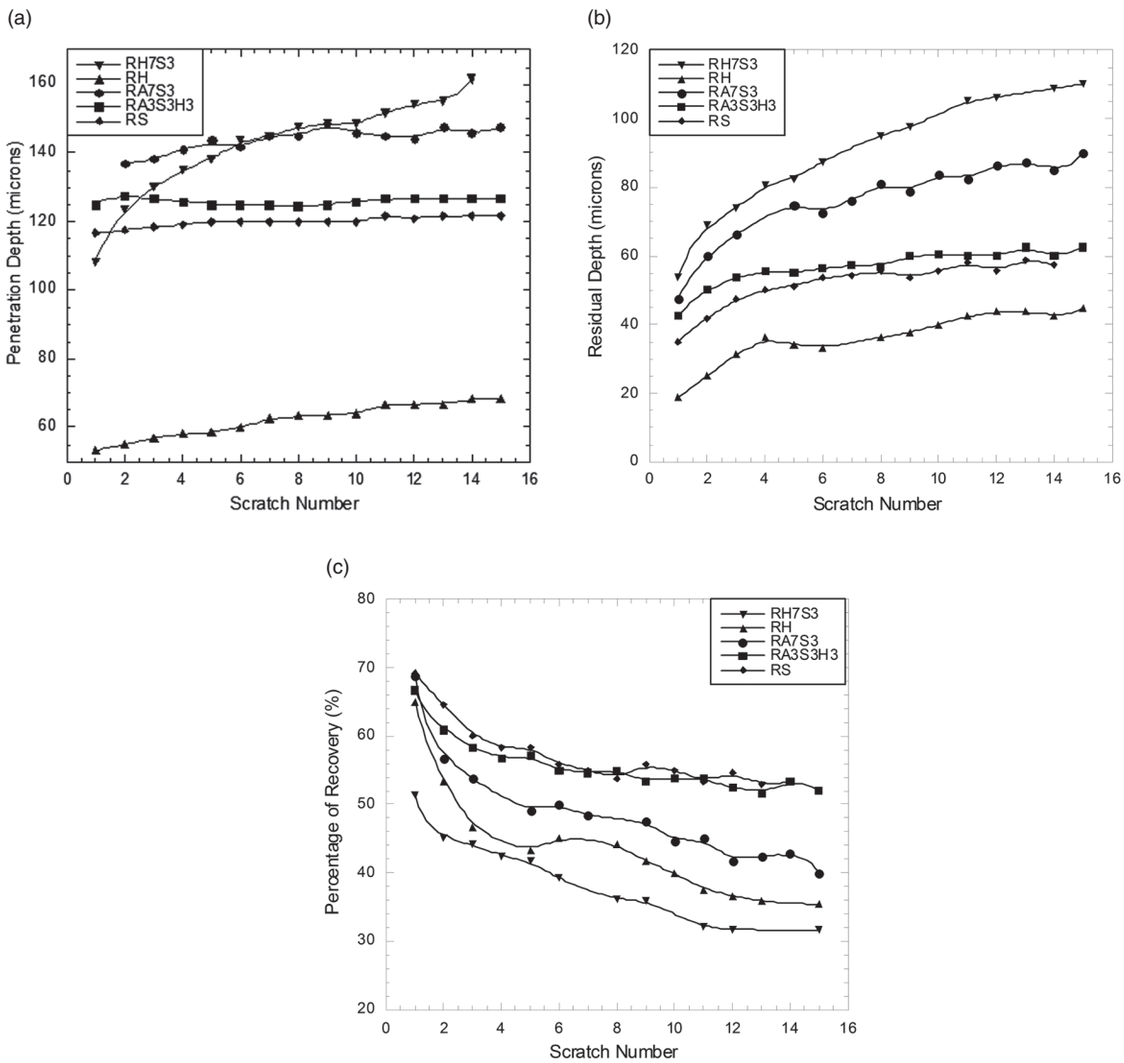

Fig. 6. Sliding wear (multi-pass scratching) as a function of the scratch number for: (a) penetration depth, (b) residual depth and (c) percentage of recovery.

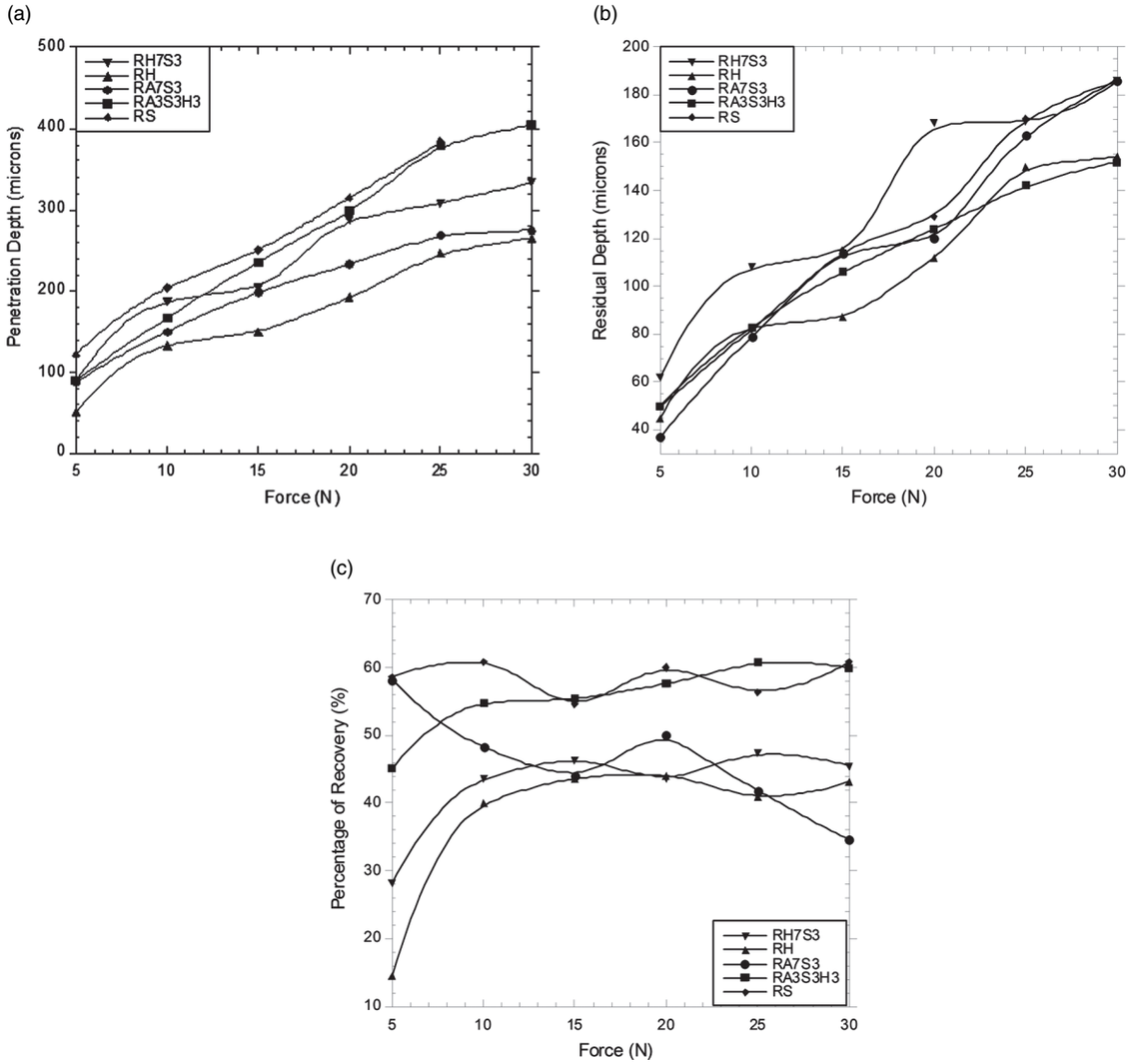

Fig. 7. Progressive scratching as a function of the force for: (a) penetration depth, (b) residual depth and (c) percentage of recovery.

RESEARCH ARTICLE

4. DISCUSSION AND CONCLUSIONS

From the optical emissions spectroscopy and FTIR, it was confirmed that the HAp used was of the correct composition and structure. In the scanning electron micrographs, we can see the effect of HAp, alumina, and silica on the porosity of the hybrid materials. The small average pore size of RH is due to the large size of the HAp particles (1.9 μm) and the comparatively low number of –OH groups that can react with the polyisocyanate and release pore forming CO_2. The combination of micro- and nanoparticles produces larger pores (in RA7S3 and RH7S3) because in these cases the number of –OH groups belonging to the ceramic particles is increased. The pore sizes of RS and RA3S3H3 are similar and just slightly larger than the pores in RH. This seems to be a result of the nano-sized particles for the former and of the combination of the three ceramics for the latter. As smaller pore size more closely mimics the properties of actual teeth,[68] the presence of HAp in combination with other sized particles seems advantageous.

The results of mechanical testing were consistent with the abrasion results. The sample containing PU resin + silica (RS) possesses the highest Young's modulus as determined from the mechanical compression tests. Likewise the sample RS had the lowest wear rate in abrasion testing. On the other hand, sample RH (containing only HAp) had the lowest modulus and highest wear rate. For the samples containing small and large ceramic particles, densification produced by the filling of the interstitial spaces improves their wear behavior over that of RH (which contains only one particle type of one size). For spheres closely packed the interstitial space is, depending on the type of packing, between 20 and 30% of the volume. Elsewhere there have been reports of improved mechanical, abrasion and other properties by addition of

silica to polymer matrices.[2, 69–71] Other fillers such as carbon nanotubes have been used for similar purposes.[72, 73] The hardness of silica and ability of the nano-sized particles to pack closely explains the high performance of the RS specimen; however this sample type lacks the HAp that improves biocompatibility and increases likelihood of tooth ingrowth.

In a broader context, Gutmanas and Gotman[74, 75] discuss importance of wear in human body replacement parts and also ways of minimizing wear in implants. In our materials the presence of HAp imparts useful properties in combination with other ceramic fillers. From Figure 6(a) showing penetration depth, we find that after the first scratch, the ceramic phase protects the material during additional scratches keeping the depth constant. The results for the residual depth, illustrated in Figure 6(b), are consistent with those in Figure 6(a) for the penetration depth. From the standpoint of aesthetics and the end use, the residual depth is the most important because it indicates the depth of the groove that will remain after a scratching event. Samples RH, RS, and RA3S3H3 had the shallowest residual depths in the multiple pass scratch tests. This is also significant as the MPS tests simulate the kind of repetitive scratching that occurs with mastication. As we examine the effect of load in the progressive scratch tests, we observe that samples RH and RA7S3 were penetrated least, meaning that these samples better support heavy loads.

In conclusion, new obturation materials were synthesized using micro- and nano-ceramic particles. Silica or alumina alone offer some improvements to mechanical and tribological properties. However, the presence of HAp is desired to improve biocompatibility. The question then is what happens in a polymer hybrid with HAp or with HAp plus additional ceramic particles. This was already addressed to some degree in 2008 (alumina with a rigid PU and HAp were best). However, that polyurethane resin required a strong solvent. A significant aspect of the present report is the use of a solvent-free PU resin as the polymer matrix. While a simple hybrid of PU + HAp performed well in scratch tests, its mechanical and abrasion properties were not as good as those of hybrids containing other ceramics. However, the hybrid containing HAp, nano-silica, and micro-alumina all together in the PU matrix stands out among the others tested. Although sample RA3S3H3 did not exhibit the highest performance in every test, overall it showed better or similar behavior to RH while also possessing a suitable morphology—a feature that was somewhat compromised in other hybrids with better mechanical properties. In summary, these composites are good candidates for obturation materials also because of the reaction between the –OH groups of dentine, HAp and the ceramic particles producing a network in the interior of the material that improves the properties and reduces micro-filtration.

Acknowledgments: The authors are in debt to Dr. Domingo Rangel for his valuable help in several of the characterization techniques used in this work, to Engineering Gerardo Fonseca for mechanical testing and to M. S. Alicia del Real for the SEM images.

References and Notes

1. K. D. Jandt and B. W. Sigusch, *Dent. Mater.* 25, 1001 (**2009**).
2. M. Estevez, S. Vargas, H. E. Hagg Lobland, A. de la Isla, W. Brostow, and R. J. Rodrıguez, *Mater. Res. Innovat.* 10, 411 (**2006**).
3. M. Estevez, S. Vargas, V. M. Castaño, J. Rogelio Rodriguez, H. E. Hagg Lobland, and W. Brostow, *Mater. Lett.* 61, 3025 (**2007**).
4. B. Bilyeu, W. Brostow, L. Chudej, M. Estevez, H. E. H. Lobland, R. J. Rodriguez, and S. Vargas, *Mater. Res. Innovat.* 11, 181 (**2007**).
5. W. Brostow, M. Estevez, H. E. Hagg Lobland, L. Hoang, J. R. Rodriguez, and S. Vargas, *J. Mater. Res.* 23, 1587 (**2008**).
6. J. W. Cho and S. H. Lee, *Eur. Polym. J.* 40, 1343 (**2004**).
7. W. E. C. Creyke, *Int. J. Mater. in Eng. Appl.* 1, 134 (**1979**).
8. B. P. Mosher, C. Wu, T. Sun, and T. Zeng, *J. Non-Cryst. Solids* 352, 3295 (**2006**).
9. G. H. Zhou, S. W. Wang, J. K. Guo, and Z. Zhang, *J. Eur. Ceram. Soc.* 28, 787 (**2008**).
10. X. L. Shi, Y. Tan, F. M. Xu, Y. L. Dong, Z. J. Zhang, X. N. Li, and L. Wang, *J. Alloys Compd.* 490, 484 (**2010**).
11. J. D. Torrey and R. K. Bordia, *J. Eur. Ceram. Soc.* 28, 253 (**2008**); E. Bernardo, P. Colombo, and S. Hampshire, *J. Eur. Ceram. Soc.* 29, 843 (**2009**).
12. A. Kopczynska and G. W. Ehrenstein, *J. Mater. Ed.* 29, 325 (**2007**).
13. V. M. Castaño and J. R. Rodriguez, Performance of Plastics, edited by W. Brostow, Hanser, Munich–Cincinnati (**2000**), Chap. 24.
14. A. Saenz, W. Brostow, E. Rivera, and V. M. Castaño, *J. Mater. Ed.* 21, 267 (**1999**).
15. A. A. Yar, M. Montazerian, H. Abdizadeh, and H. R. Baharvandi, *J. Alloys Compd.* 484, 400 (**2009**).
16. V. Rajkovic, D. Bozic, and M. T. Jovanovic, *J. Alloys Compd.* 459, 177 (**2008**).
17. L. G. Hanu, G. P. Simon, J. Mansouri, R. P. Burford, and Y. B. Cheng, *J. Mater. Proc. Technol.* 153–154, 401 (**2004**).
18. S. Varghese, J. Karger-Kocsis, and K. G. Gatos, *Polymer* 44, 3977 (**2003**).
19. W. S. Chow, Z. A. Mohd Ishak, J. Karger-Kocsis, A. A. Apostolov, and U. S. Ishiaku, *Polymer* 44, 7427 (**2003**).
20. W. Brostow, B. P. Gorman, and O. Olea-Mejia, *Mater. Lett.* 61, 1333 (**2007**).
21. W. Brostow, A. Buchman, E. Buchman, and O. Olea-Mejia, *Polym. Eng. Sci.* 48, 1977 (**2008**).
22. W. Brostow and T. Datashvili, *Chem. Chem. Tech.* 2, 27 (**2008**).
23. W. Brostow, T. Datashvili, D. Kao, and J. Too, *Polym. Compos.* 31, 417 (**2010**).
24. D. C. Southam, T. W. Lewis, A. J. McFarlane, T. Borrmann, and J. H. Johnston, *J. Colloid Interface Sci.* 319, 489 (**2008**).
25. T. V. Safronova, V. I. Putlyaev, M. A. Shekhirev, Y. D, Tretyakov, A. V. Kuznetsov, and A. V. Belyakov, *J. Eur. Ceram. Soc.* 29, 1925 (**2009**).
26. G. Zhang, J. Karger-Kocsis, and J. Zou, *Carbon* 48, 4289 (**2010**).
27. D. S. dos Santos, Jr., P. J. G. Goulet, N. P. W. Pieczonka, O. V. Oliveira, Jr., and R. F. Aroca, *Langmuir* 20, 10273 (**2004**).
28. S. Huang, K. Zhou, B. Huang, Z. Li, S. Zhu, and G. Wang, *J. Mater. Sci. Med.* 19, 437 (**2008**).
29. L. H. Mair, T. A. Stolarski, R. W. Vowles, and C. H. Lloyd, *J. Dentistry* 24, 141 (**1996**).
30. I. About, P. E. Murray, J.-C. Franquin, M. Remusat, and A. J. Smith, *J. Dentistry* 29, 109 (**2001**).

RESEARCH ARTICLE

31. Y.-R. Jeng, T.-T. Lin, and D.-B. Shieh, *J. Biomechanics* 42, 2249 **(2009)**.
32. M.-S. Choi, Y.-K. Lee, B.-S. Lim, S.-H. Rhee, and H.-C. Yang, *J. Mater. Sci. Med.* 16, 347 **(2005)**.
33. S. He, Q. Liu, Y.-W. Mai, and R. Bryant, *J. Mater. Sci. Med.* 7, 611 **(1996)**.
34. W. Brostow, H. E. Hagg Lobland, and M. Narkis, *J. Mater. Res.* 21, 2422 **(2006)**.
35. W. Brostow and H. E. H. Lobland, *J. Mater. Sci.* 45, 242 **(2010)**.
36. S. Boutaleb, F. Zaïri, A. Mesbah, M. Naït-Abdelaziz, J. M. Gloaguen, T. Boukharouba, and J. M. Lefebvre, *Int. J. Solids Structures* 46, 1716 **(2009)**.
37. M. Z. Rong, Q. L. Ji, M. Q. Zhang, and K. Friedrich, *Eur. Polym. J.* 38, 1573 **(2002)**.
38. Y. Hashimoto, Y. Moriguchi, H. Oshima, J. Nishikawa, T. Nishihara, and M. Nakamura, *J. Mater. Sci. Med.* 11, 465 **(2000)**.
39. N. A. Chowdhury, K. Wakasa, R. Priyawan, and M. Yamaki, *J. Mater. Sci. Med.* 8, 149 **(1997)**.
40. C. D. Mayworm, S. S. Camargo, Jr., and F. L. Bastian, *J. Dentistry* 36, 703 **(2008)**.
41. G. Guidoni, M. Swain, and I. Jäger, *J. Dentistry* 36, 786 **(2008)**.
42. E. Pissiotis and L. S. W. Spångberg, *J. Endodontics* 16, 468 **(1990)**.
43. A. G. Mamalis, G. L. Petrossian, and D. E. Manolakos, *J. Mat. Proc. Technol.* 148, 382 **(2004)**.
44. H. Tai, A. Sergienko, and M. S. Silverstein, *Polym. Eng. Sci.* 41, 1540 **(2001)**; H. Tai, A. Sergienko, and M. S. Silverstein, *Polymer* 42, 4473 **(2001)**.
45. A.-A. A. Abdel Azim, A. M. Abdel-Raheim, A. M. Atta, W. Brostow, and A. F. El-Kafrawy, *e-Polymers* no. 118 **(2007)**.
46. S. Livshin and M. S. Silverstein, *Macromolecules* 40, 6349 **(2007)**; J. Normatov and M. S. Silverstein, *J. Polym. Sci. Chem.* 46, 2357 **(2008)**.
47. A.-A. A. Abdel-Azim, A. M. Abdul-Raheim, A. M. Atta, W. Brostow, and T. Datashvili, *e-Polymers* no. 134 **(2009)**.
48. I. Gurevitch and M. S. Silverstein, *J. Polym. Sci. Chem.* 48, 1516 **(2010)**.
49. Z. Kadirova, Y. Kameshima, A. Nakajima, and K. Okada, *J. Haz. Mater.* 137, 352 **(2006)**.
50. J. R. Diaz, E. Rivera-Muñoz, W. Brostow, and V. M. Castaño, *J. Mater. Sci. Med.* 12, 305 **(2001)**.
51. M. Ilavský, H. W. Ulmer, K. te Nijenhuis, and W. J. Mijs, *Eur. Polym. J.* 37, 887 **(2001)**.
52. A. Mirčeva, M. Janežič, M. Žigon, and T. Malavašič, *J. Molec. Struct.* 267, 129 **(1992)**.
53. M. Gelinsky, P. B. Welzel, P. Simon, A. Bernhardt, and U. König, *Chem. Eng. J.* 137, 84 **(2008)**.
54. D. J. A. Netz, P. Sepulveda, V. C. Pandolfelli, A. C. C. Spadaro, J. B. Alencastre, M. V. L. B. Bentley, and J. M. Marchetti, *Int. J. Pharmaceutics* 213, 117 **(2001)**.
55. N. Guermazi, K. Elleuch, H. F. Ayedi, Ph. Kapsa, *J. Mater. Proc. Technol.* 203, 404 **(2008)**.
56. H.-J. Song, Z.-Z. Zhang, and X.-H. Men, *Eur. Polym. J.* 44, 1012 **(2008)**.
57. I. Mobasherpour, M. Soulati Heshajin, A. Kazemzadeh, and M. Zakeri, *J. Alloys Compd.* 430, 330 **(2007)**.
58. M. Vorbau, L. Hillemann, and M. Stintz, *J. Aerosol Sci.* 40, 209 **(2009)**.
59. W. Brostow, B. Bujard, P. E. Cassidy, H. E. Hagg, P. E. Montemartini, *Mater. Res. Innovat.* 6, 7 **(2002)**; W. Brostow, J.-L. Deborde, M. Jaklewicz, and P. Olszynski, *J. Mater. Ed.* 25, 119 **(2003)**; W. Brostow, V. Kovacevic, D. Vrsaljko, and J. Whitworth, *J. Mater. Ed.* 32, 273 **(2010)**.
60. W. Brostow, W. Chonkaew, L. Rapoport, Y. Soifer, and A. Verdyan, *J. Mater. Res.* 22, 2483 **(2007)**.
61. W. Brostow, W. Chonkaew, S. Mirshams, and A. Srivastava, *Polym. Eng. Sci.* 48, 2060 **(2008)**.
62. W. Brostow, G. Damarla, J. Howe, and D. Pietkiewicz, *e-Polymers* no. 025 **(2004)**.
63. M.-D. Bermudez, W. Brostow, F. J. Carrion-Vilches, J. J. Cervantes, and D. Pietkiewicz, *e-Polymers* no. 001 **(2005)**.
64. S. M. Rabiee, F. Moztarzadeh, and M. Solati-Hashjin, *J. Molec. Struct.* 969, 172 **(2010)**.
65. G. Gregori, H.-J. Kleebe, H. Mayr, and G. Ziegler, *J. Eur. Ceram. Soc.* 26, 1473 **(2006)**.
66. N. Ozgür Engin and A. Cüneyt Tas, *J. Eur. Ceram. Soc.* 19, 2569 **(1999)**.
67. G. S. Kumar, E. K. Girija, A. Thamizhavel, Y. Yokogawa, and S. Narayana Kalkura, *J. Colloid Interface Sci.* 349, 56 **(2010)**.
68. R. Schilke, J. A. Lisson, O. Baub, and W. Geurtsen, *Arch. Oral Biol.* 45, 355 **(2000)**.
69. W. Brostow, T. Datashvili, and K. P. Hackenberg, *e-Polymers* no. 054 **(2008)**.
70. W. Brostow, W. Chonkaew, T. Datashvili, and K. P. Menard, *J. Nanosci. Nanotech.* 8, 916 **(2008)**.
71. A. F. Vargas, W. Brostow, H. E. Hagg Lobland, B. L. Lopez, and O. Olea-Mejia, *J. Nanosci. Nanotech.* 9, 6661 **(2009)**.
72. A. Nogales, G. Broza, Z. Roslaniec, K. Schulte, I. Sics, B. S. Hsiao, A. Sanz, M. C. Garcia-Gutierrez, D. R. Rueda, C. Domingo, and T. A. Ezquerra, *Macromolecules* 37, 7669 **(2004)**.
73. G. Broza and K. Schulte, *Polymer Eng. Sci.* 48, 2033 **(2008)**.
74. E. Y. Gutmanas and I. Gotman, *J. Mater. Sci. Med.* 15, 327 **(2004)**.
75. I. Mashal, L. Klinger, I. Gotman, and E. Y. Gutmanas, *Surface Coatings Tech.* 200, 3561 **(2006)**.

Received: 7 November 2010. Accepted: 10 February 2011.

RESEARCH ARTICLE